Hindawi Publishing Corporation
Journal of Biomedicine and Biotechnology
Volume 2009, Article ID 924565, 12 pages
doi:10.1155/2009/924565

Methodology Report

Gene Expression Analysis of an *EGFR* Indirectly Related Pathway Identified *PTEN* and *MMP9* as Reliable Diagnostic Markers for Human Glial Tumor Specimens

Sergio Comincini,[1] Mayra Paolillo,[2] Giulia Barbieri,[1] Silvia Palumbo,[1] Elena Sbalchiero,[1] Alberto Azzalin,[1] Marika A. Russo,[2] and Sergio Schinelli[2]

[1] *Dipartimento di Genetica e Microbiologia, Università di Pavia, Via Ferrata 1, 27100 Pavia, Italy*
[2] *Dipartimento di Farmacologia Sperimentale ed Applicata, Università di Pavia, Viale Taramelli 14, 27100 Pavia, Italy*

Correspondence should be addressed to Sergio Comincini, sergio.c@ipvgen.unipv.it

Received 9 February 2009; Revised 23 April 2009; Accepted 18 May 2009

Recommended by Zhumur Ghosh

In this study the mRNA levels of five *EGFR* indirectly related genes, *EGFR*, *HB-EGF*, *ADAM17*, *PTEN*, and *MMP9*, have been assessed by Real-time PCR in a panel of 37 glioblastoma multiforme specimens and in 5 normal brain samples; as a result, in glioblastoma, *ADAM17* and *PTEN* expression was significantly lower than in normal brain samples, and, in particular, a statistically significant inverse correlation was found between *PTEN* and *MMP9* mRNA levels. To verify if this correlation was conserved in gliomas, *PTEN* and *MMP9* expression was further investigated in an additional panel of 16 anaplastic astrocytoma specimens and, in parallel, in different human normal and astrocytic tumor cell lines. In anaplastic astrocytomas *PTEN* expression was significantly higher than in glioblastoma multiforme, but no significant correlation was found between *PTEN* and *MMP9* expression. *PTEN* and *MMP9* mRNA levels were also employed to identify subgroups of specimens within the different glioma malignancy grades and to define a gene expression-based diagnostic classification scheme. In conclusion, this gene expression survey highlighted that the combined measurement of *PTEN* and *MMP9* transcripts might represent a novel reliable tool for the differential diagnosis of high-grade gliomas, and it also suggested a functional link involving these genes in glial tumors.

1. Introduction

Glioblastoma multiforme is the most malignant brain tumor among astrocytic gliomas with a typical prognosis of about 12 months in spite of current therapeutic approaches that include neurosurgery followed by combined chemotherapy and radiotherapy [1]. Recently, the development of massive screening genome technologies, such as gene expression profiling, has prompted new attempts to the classification of glioblastoma subgroups on molecular basis in order to identify new diagnostic or prognostic tools. At present the search for potential molecular markers among aberrant signal transduction pathways in glioblastoma is actively exploited for the optimization of existing therapies or the development of innovative drugs [2]. However, the accomplishment of this ambitious task is severely hindered by the extreme heterogeneity of glioblastoma tumor samples and by the subsequent variability of possibly identified molecular markers. One way to overcome this limit could be represented by the concomitant analysis of the mRNA expression of several selected genes, already known to be functionally involved in the cellular malignant transformation. This analysis could highlight differences in gene expression levels among high-grade gliomas, or at the same time it could reveal relationships within glioma subtypes between the genes analyzed in order to improve their reliability as prognostic or diagnostic markers.

The epidermal growth factor (EGF) receptor (EGFR or ErbB1) plays a pivotal role in cancer physiology because its activation, elicited by at least six different endogenous peptidergic EGF-like ligands, leads to the activation of intracellular signalling pathways that modulate cell

Table 1: Age, gender, mRNA expression values (in femptograms), and anatomical location of glioblasytoma multiforme samples.

Age	Sex	*EGFR*	*ADAM17*	*HB-EGF*	*PTEN*	*MMP9*	Location
68	M	2.78	0.31	0.69	1.85	6.39	Parietal
84	F	155.97	0.31	4.43	6.81	31.13	Parietal
23	M	95.25	3.54	19.01	5.15	0.04	Cerebellum
50	M	579.69	0.87	9.28	8.97	43.32	Frontal dx
71	F	7.11	0.08	0.82	2.27	0.21	Frontal dx
58	M	236.18	0.91	8.98	15.05	183.29	Parietal dx
66	M	12.85	0.13	1.38	0.41	0.04	Temporal sx
50	M	150.97	3.08	4.87	1.65	3.09	Temporal dx
38	F	60.10	2.23	9.23	7.01	30.41	Occipital dx
61	F	2.88	0.41	1.75	1.96	0.72	Frontal sx
68	F	4.87	0.63	8.71	0.82	0.82	Occipital dx
70	M	23.38	2.13	2.82	3.92	3.51	Frontal dx
59	M	425.51	1.28	4.32	4.84	8.04	Frontal sx
67	F	1268.24	2.99	13.92	12.68	32.58	Temporal dx
31	M	13.33	1.87	52.08	6.66	13.33	Frontal sx
68	F	0.77	0.59	12.85	0.62	1.04	Parietal dx
39	F	6.87	13.33	0.21	3.14	0.16	Frontoinsular
39	M	2.37	0.42	3.96	4.79	0.21	Parietal sx
45	F	274.74	0.66	7.14	1.25	2.52	Frontal dx
63	M	1284.37	13.33	0.21	3.12	10.62	Temporal dx
71	M	30.11	5.42	10.62	2.92	2.08	Frontal sx
60	M	73.96	17.71	7.54	3.33	4.37	Temporal sx
44	F	2562.92	6.87	18.96	3.33	8.33	Thalamus sx
73	F	38.75	13.12	7.53	3.33	1.04	Paratrigonal sx
47	F	16.88	4.79	7.29	3.13	1.04	Frontal sx
63	M	12.01	12.31	28.22	3.85	3.28	Occipital dx
77	F	239.85	8.72	22.56	2.92	6.31	Cortical anterior
55	F	22.36	2.51	5.38	1.54	0.05	Parietal dx
70	F	13.18	9.18	12.31	3.08	0.16	Parietal dx
60	F	8.92	7.95	16.56	1.54	0.23	Temporal sx
54	M	1071.43	15.49	16.56	2.56	1.64	Temporal sx
55	M	371.49	9.54	19.49	1.54	1.85	Temporal sx
55	F	27.54	9.23	5.13	1.54	0.15	Temporal sx
58	M	21.38	20.87	17.38	3.08	1.23	Temporal sx
53	F	8.1	7.23	9.74	2.05	0.15	Occipital sx
69	F	4.66	12.56	26.69	3.08	1.69	Frontal sx
70	F	29.49	5.23	7.08	7.23	0.61	Parietal dx

proliferation, metastasis, and angiogenesis [3]. About 40%–50% of glioblastoma cases are characterized by *EGFR* gene amplification or overexpression, together with the expression of the mutated and constitutively active EGFR isoform EGFRvIII [3]. Upregulation of the EGFR pathway could also result from an increased availability of EGFR endogenous agonists belonging to the family of EGF-like growth factors.

Heparin-binding epidermal growth factor (HB-EGF) acts as a potent proliferative agent in many different cell types via the activation of EGFR or the other EGF-like receptor ErbB4 [4]. HB-EGF is initially synthesized as the membrane-spanning protein proHB-EGF and then is proteolytically cleaved by "A *D*isintegrin *A*nd *M*etalloproteinase" (ADAM) family members that release the soluble form (sHB-EGF) in the extracellular space. The ADAM isoform responsible for this process appears to be cell type dependent, since in different experimental models ADAM 10, 12, and 17 have been involved in proHB-EGF shedding [3]. The overexpression of ADAM17, also named "tumor necrosis factor-alpha-converting enzyme" (TACE), seems to be involved in the malignant potential of cancer cells [5], and, notably, this metalloprotease modulates HB-EGF shedding and cell proliferation in U373-MG glioblastoma cell line [5].

In the clinical practice only 10%–20% of glioblastoma patients respond to EGFR kinase inhibitors, and this poor response has been ascribed to a combination of EGFR

Table 2: Age, gender, *PTEN*, and *MMP9* expression values (in femtograms), and anatomical location of anaplastic astrocytoma samples.

Age	Sex	*PTEN*	*MMP9*	Location
44	M	1.72	1.25	Temporal sx
68	F	7.66	0.57	Thalamus sx
67	F	2.25	37.06	Frontal dx
60	F	2.44	1.62	Frontal sx
50	M	92.46	0.79	Temporal dx
39	M	79.25	32.92	Parietal dx
64	F	33.82	43.21	Parietal dx
28	F	25.64	26.24	Temporal sx
55	F	12.47	0.32	Temporal sx
31	M	19.81	1.95	Temporal sx
52	F	50.12	4.37	Temporal sx
71	F	17.98	0.28	Frontal cortex
62	M	20.41	0.03	Total cortex
50	M	60.72	0.76	Occipital cortex
52	M	45.11	0.45	Total cortex
68	F	25.30	0.23	Frontal cortex

Table 3: Age, gender, mRNA expression values (in femtograms), and anatomical location of normal brain specimens.

Age	Sex	*EGFR*	*ADAM17*	*HB-EGF*	*PTEN*	*MMP9*	Location
71	F	32.58	10.74	14.84	17.98	0.28	Frontal cortex
62	M	16.70	12.76	10.41	20.41	0.03	Total cortex
50	M	57.94	18.35	30.41	60.72	0.76	Occipital cortex
52	M	25.74	13.87	28.55	45.11	0.45	Total cortex
68	F	46.98	17.20	7.60	25.30	0.23	Frontal cortex

Table 4: *MMP9* and *PTEN* absolute quantitative expression in different human normal (NHA) and glioma (PRT-HU2 and U138-MG) cell lines. Expression is indicated in femptograms.

Cell line	*MMP9*	*PTEN*
NHA	0.59	117.97
PRT-HU2	0.56	45.62
U138-MG	3.09	4.08

overexpression and loss or mutation of the Phosphatase and TEN sin homolog deleted from chromosome 10 (PTEN) tumor suppressor protein [6]. The PTEN phosphatase reduces the levels of the second messenger phosphatidylinositol 3,4,5-triphosphate (PI3K) and regulates the activity of the downstream PI-3K/AKT- and mammalian target of rapamacyn- (mTOR-) dependent pathways [7]. Notably, PTEN functional loss or mutation is present in 60%–70% of high-grade gliomas and is associated with malignant phenotypic changes such as migration capability, probably by modulation of FAK activity [8]. Moreover, since PTEN loss appears to accelerate the formation of high-grade gliomas [6], it could potentially represent a valid candidate gene to discriminate between high- and low-grade gliomas.

One typical feature of glioblastoma is its high ability to disseminate and spread to distant brain areas. Proteases expressed by glioma cells appear to play a significant role in these processes because selective matrix metalloproteinases like MMP2 or MMP9 degrade the extracellular environment in order to facilitate tumor cell growth and migration. Expression of these proteases appears to increase with glioma grade and in vitro studies showed that modifications of their expression levels resulted in altered migratory properties [9]. Although some previous reports have examined the expression of EGFR [3], PTEN [10], HB-EGF [9], ADAM17 [11], and MMP9 [12] in astrocytoma samples, at present the transcriptional expression of these five EGFR pathway-related genes has not yet been simultaneously investigated in glioma.

Therefore, in this study we have evaluated by quantitative Real-time PCR the expression of *ADAM17*, *EGFR*, *HB-EGF*, *PTEN*, and *MMP9* mRNAs in a panel of glioblastoma and anaplastic astrocytomas specimens and cell lines, and we have finally compared them to normal control samples to ascertain whether these expression profiles might provide additional tools in glioma diagnosis and in tumor subtypes identification.

2. Materials and Methods

2.1. Human Biopsy Samples. Biopsy samples, obtained from Azienda Ospedaliera Universitaria di Parma (Parma, Italy) after informed consent of the patients, were placed in ice-cold Trizol reagent (Invitrogen, Paisley, UK) and immediately processed for RNA extraction. Sections of samples were

Table 5: GeneBank accession numbers, PCR primer sequences, and products.

Gene	Accession number	PCR primer sequences (5′-3′)	PCR product (bp)
EGFR	NM_005228	AGGAAGAAGCTTGCTGGTAGC CTCTGGAAGACTTGTGGCTTG	88
ADAM17	NM_003183	CAAGTCATTTGAGGATCTCACG TCTTTGCTGTCAACACGATTCT	96
HB-EGF	NM_001945	GCCTAGGCGATTTTGTCTACC GCCCAACCTCTTCTGAGACTT	119
PTEN	NM_000314	CAGCAGTGGCTCTGTGTGTAA ATGGACATCTGATTGGGATGA	98
MMP9	NM_004994	AAAGCCTATTTCTGCCAGGAC GCACTGCAGGATGTCATAGGT	105

independently histologically and morphologically evaluated by different neuropathologists and classified as grade IV (glioblastoma multiforme) or grade III (anaplastic astrocytoma), according to WHO guidelines [13]. Clinical data of glioblastoma patients are reported in Table 1, and they included 19 females and 18 males (age range 23–84 years, mean 57.8 ± 13.3). The anaplastic astrocytoma patients (Table 2) included 7 males and 9 females (age 28–68, mean 50.7 ± 13.9). Total RNA samples extracted from human postmortem normal brain (NB) cortical regions, as reported in Table 3, were purchased from Ambion (Foster City, Calif, USA): these included 2 females and 3 males (age range 50–71 years, mean 60.6 ± 9.3).

2.2. Cell Lines. Normal human astrocytes (NHAs) were purchased from Cambrex (East Rutherford, NJ, USA) and cultivated in the specific astrocyte AGM medium (Cambrex) according to the manufacturer's specifications. Human glioma cell line U138-MG, derived from a glioblastoma multiforme patient and widely employed, was purchased from ATCC (Rockville, Md, USA); PRT-HU2 cells, previously described [14], were analogously derived from a glioblastoma multiforme patient. U138-MG and PRT-HU2 cells were cultivated in D-MEM medium supplemented with 10% FBS, 100 units/mL penicillin, 0.1 mg/mL streptomycin, and 1% L-glutamine (Invitrogen, Paisley, UK).

2.3. Real Time Quantitative PCR. Total RNA was extracted as previously described [14] and accurately quantified using spectrophotometric and fluorimetric (Quant-it RNA Assay, Invitrogen) approaches. The gene-specific primers were designed using the "Primer3 input" software (http://frodo.wi.mit.edu/primer3/), and their specificity was verified using the Primer-BLAST software (http://www.ncbi.nlm.nih.gov/tools/primer-blast/index.cgi?LINK_LOC=BlastHome/). GeneBank accession numbers of the five genes examined, their respective primer pairs sequences, and PCR products lengths were reported in Table 5. Quantitative Real-time PCR analysis was performed as previously described [14]. For the absolute quantification of specific cDNA, standard curves were derived using different concentrations of *EGFR*, *ADAM17*, *MMP9*, *HB-EGF*, and *PTEN* DNA-sequenced templates, prepared by reamplifying the PCR purified products obtained from Real-time PCR. The second derivative maximum method in the Light Cycler software was used to calculate the crossing point (Cp) value, and the concentrations of each specific cDNA were determined. All results were quantitative expressed in femtograms (fg) of cDNA, normalized to a total RNA input of 1 microgram.

2.4. Statistical and Bioinformatics Analysis. All results were expressed as mean ± standard deviation of each biopsy specimens, assayed in duplicate. The Instat v.3 software (GraphPad Software Inc., Mass, USA) was used for the statistical analysis of differences in gene expression between groups by one-way ANOVA and for the analysis of correlations among gene expression profiles, using the Pearson coefficient r. A P-value less than .05 was considered statistically significant. The dendrogram and the classification tree analysis were performed using the Orange data mining software (http://www.ailab.si/orange/). In particular, for the hierarchical clustering analysis, an Euclidean distance matrix was adopted. Statistical trends were obtained from the *PTEN* and *MMP9* average quantitative expression within normal control, anaplastic astrocytoma, and glioblastoma multiforme diagnostic classes, using the Excel software with an exponential setting (Microsoft Word Package 2003, Redmond, Wash, USA).

3. Results

The mRNA expression of the investigated genes of glioblastoma multiforme and normal brain specimens were analytically reported in Tables 1 and 2 and depicted in Figures 1 and 2. On the basis of their expression patterns in glioblastoma and using the mean values of normal samples as cut-off, the investigated genes were roughly classified in three different subgroups, the first including *ADAM17, HB-EGF*, and *PTEN*, whose average levels in glioblastoma were below the controls, the second comprising *MMP9,* whose majority of values in glioblastoma specimens were higher than in controls and, finally, the last one constituted by the *EGFR* gene, displaying the widest variation and data dispersion (Figure 1).

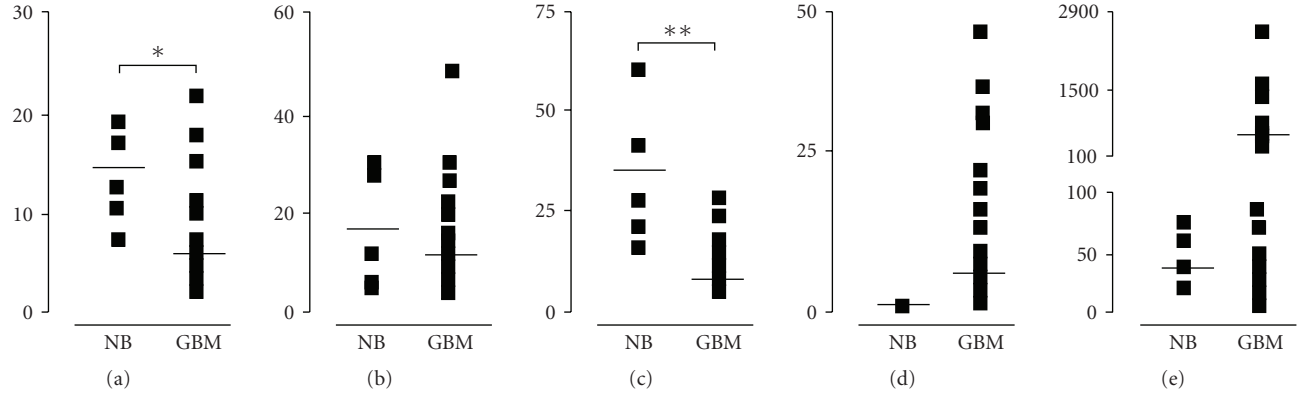

Figure 1: The mRNA expression levels of (a) *ADAM17*, (b) *HB-EGF*, (c) *PTEN*, (d) *MMP9*, and (e) *EGFR* in 37 human glioblastoma samples (GBM) and in five normal brain cortex samples (NB). Horizontal lines represent the mean values. $^{*}P < .002$, $^{**}P < .0001$.

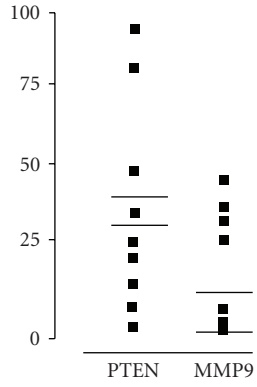

Figure 2: The mRNA expression levels of *PTEN* and *MMP9* in 16 human grade III astrocytoma samples (AA). Bold horizontal lines represent the mean values, and thin lines represent the mean normal brain cortex samples (NB) values.

The mRNA levels of *ADAM17* metallo-protease in glioblastoma (mean 5.88 fg ± 5.71) were significantly lower ($P < .002$) than in controls (14.51 fg ± 3.15). In particular, in 33 out of 37 cases (89.19%), *ADAM17* expression was lower than in control samples. For *HB-EGF* gene, although 31 out of 37 (83.78%) glioblastoma samples displayed mRNA levels lower than controls, statistical analysis revealed that the difference between controls (18.36 fg ± 10.52) and glioblastoma specimens (10.96 fg±10.13) was not statistically significant ($P < .434$).

PTEN expression pattern showed statistically lower mRNA levels in all glioblastoma samples compared to controls. Notably, the highest *PTEN* expression level among all glioblastoma had a quantitative expression (15.05 fg) that was less than 50% of the mean controls values (33.91 fg), with a control normalized ratio ranging from 2.25 to 82.72 fg. As expected, there was a very high statistically significant difference ($P < .0001$) of *PTEN* mRNA expression between glioblastoma (3.86 fg ± 3.15) and controls (33.91 fg ± 18.44).

MMP9 was overexpressed in the majority of glioblastoma specimens (72.22%) and, furthermore, in a subgroup of 24 cases (64.86%) the expression level was at least twofold higher than in controls, with a control normalized ratio within this subgroup ranging from 1.74 to 123.71 fg. However, the mean expression level of *MMP9* mRNA in glioblastoma (5.11 fg ± 8.78) was not significantly different ($P = .238$) from control samples (0.35 fg ± 0.27).

EGFR mRNA transcript levels, due to their amplitude in expression, were arbitrarily divided into two glioblastoma subgroups. The former, ranging from 0.77 to 95.25 fg, included 25 samples (67.63%); the latter, had *EGRF* absolute quantitative values ranging from 150.97 to 2562.92 fg. All control samples showed *EGFR* expression values below 100 fg, with a mean value of 35.98 fg ± 16.51. It was evident that for *EGFR* there was no statistically significant difference ($P < .371$) between glioblastoma (247.60 fg ± 517.45) and control samples (35.98 fg ± 16.52).

Within glioblastoma samples, a highly statistically significant negative correlation ($P < .0001$; Person coefficient $r = -0.776$) was related to the expression of *PTEN* and *MMP9*; in a different manner, a statistically significant positive correlation ($P < .05$; Pearson coefficient, $r = 0.9221$) was scored for the same genes within the control samples. The inverse correlation found between *PTEN* and *MMP9* mRNA expression in glioblastoma compared to control samples, prompted us to investigate whether this correlation was also detectable in other glioma grades of malignancy. Therefore, *PTEN* and *MMP9* expression, reported in Table 2 and illustrated in Figure 2, was investigated in 16 histological confirmed anaplastic astrocytoma specimens, previously classified as WHO grade III. In these samples, *PTEN* mRNA normalized quantitation (29.72 fg ± 31.62) was not significantly different from control ($P = .792$), but this value was significantly higher compared to glioblastoma ($P < .0001$). *MMP9* expression (13.60 fg ± 17.28) was neither significantly different from the control (0.35 fg ± 0.27, $P = .113$) nor from glioblastoma specimens ($P = .103$). Notably, no statistically significant correlation ($P = .709$) was found between the mRNA levels of these two genes in anaplastic astrocytoma samples. Differently from glioblastoma, no inverse correlation in *PTEN* and *MMP9* expression was found comparing anaplastic astrocytoma and control samples (Pearson coefficient, $r = 0.127$).

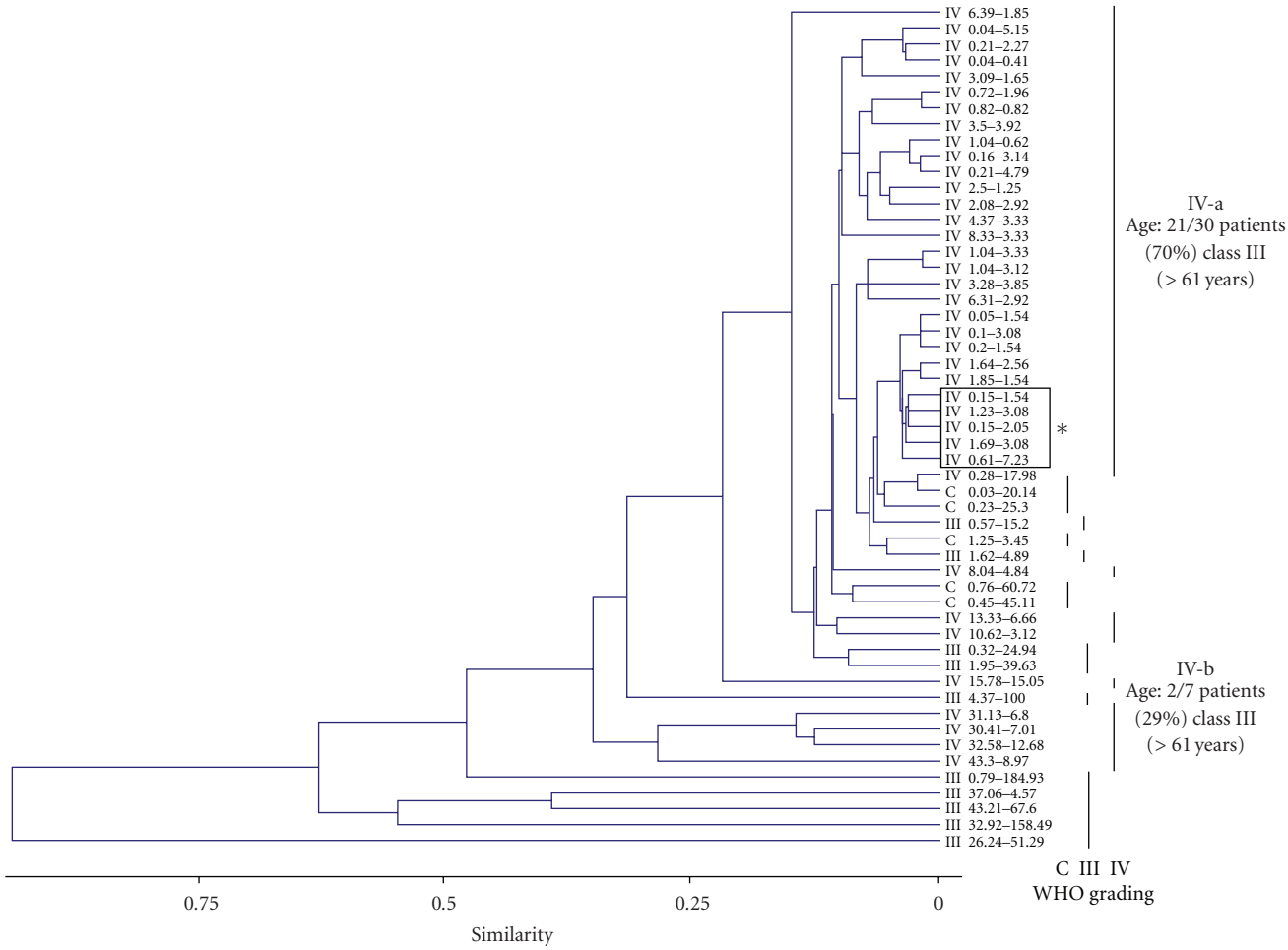

Figure 3: Dendrogram comparing *PTEN* and *MMP9* absolute quantitative expression. Absolute quantifications are expressed in femtograms, as reported in Materials and Methods. WHO grades of malignancy (III, IV) and healthy brain control (C) specimens are indicated. Glioblastoma multiforme subgroups IV-a, including the majority of glioblastoma specimens, and IV-b, described in Results, are highlighted. The box (∗) indicates subgrouping of patients sharing similar tumor anatomical localization (i.e., temporal). Subgroups IV-a and IV-b have a different and significant distribution of age-class III patients (>61 years, $P < .01$ Anova-one way).

Then, *PTEN* and *MMP9* mRNA levels were comparatively examined in two different human established glioblastoma cell lines (PRT-HU2 and U138-MG) and in a primary culture of embryonic normal human astrocytes (NHA), as shown in Table 4. In these cells, *PTEN* mRNA levels were much variable comparing to *MMP9* expression; similarly to the above examined control samples, normal astrocytes exhibited the highest *PTEN* expression.

We next exploited if *PTEN* and *MMP9* expression might be more tightly related to the glioma tumor progression. To this purpose, different bioinformatics analyses were performed using the experimental data set reported in Tables 1, 2, 3, and 4 and considering the WHO grading of the specimens. We therefore performed hierarchical clustering, a standard unsupervised learning method [10] of the tumor specimens. The WHO grading was simultaneously compared to *PTEN* and *MMP9* expression values, to identify homogeneous clusters. As reported in the dendrogram of Figure 3, different groups of samples were created, according to the above mentioned criteria. Using Euclidean distances, WHO grades IV and III and normal control samples were roughly classified into different clusters. Of note, a major subset of the glioblastoma specimens was identified (Figure 3, subgroup IV-a), showing the lowest and almost similar levels of both *PTEN* and *MMP9* transcripts; the remaining glioblastoma samples clustered within subgroup IV-b. The association of tumor anatomical localization and age of the patients with the levels of *PTEN* and *MMP9* expression was also investigated. According to the clinical data (Tables 1–3), ages of the patients were divided into three classes (i.e., I, 20–40; II, 41–60; III, >61 years): as reported in the dendrogram, the age-class III patients exhibited a statistically significant difference in distribution between subgroups IV-a and IV-b ($P < .01$, Anova one-way). Differently, no clear associations between levels of *PTEN* and *MMP9* expression and tumor localization were highlighted, with the exception of a single cluster of four class-III patients with a temporal tumor localization within subgroup IV-a.

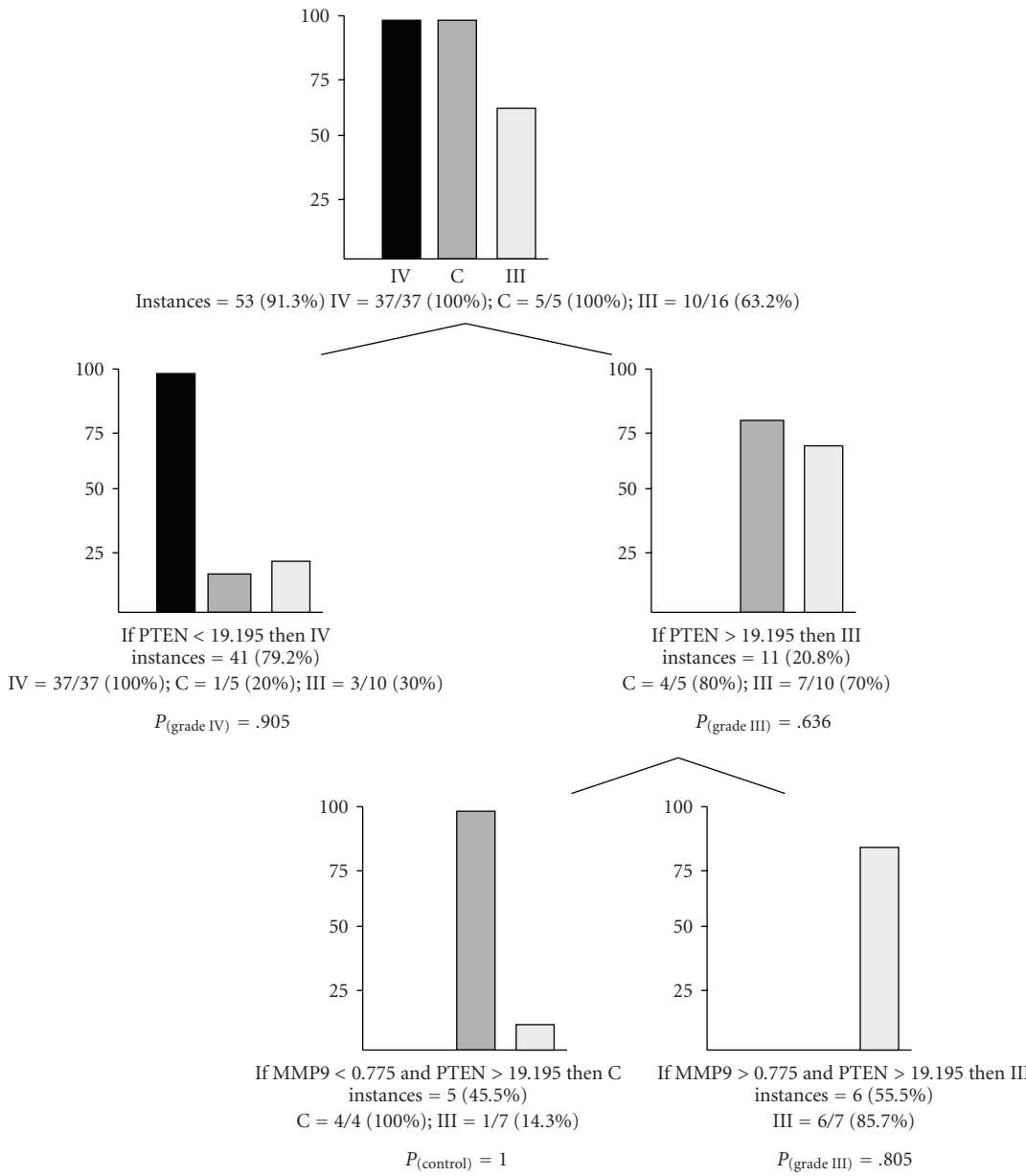

Figure 4: Classification tree derived from the combined measurement of *PTEN* and *MMP9* quantitative expression. At each root, diagnostic classes are divided following the absolute quantification and expressed in femtograms. Probabilities values (P) for the different classes are reported.

Then, a classification tree was produced, evaluating the performance of *PTEN* and *MMP9* expression in predicting roots characterized by different WHO malignant grades; as reported in Figure 4, 53 out of 58 total samples, corresponding to 53 instances (i.e., 91.3%) fitted with the classification tree; in detail, all grade IV samples had *PTEN* normalized expression values below a quantity of 19.195 fg (37/37 instances, $P = .905$), while the large majority of control (80% of the total C instances) and anaplastic astrocytomas samples (70%, $P = .636$) were grouped with *PTEN* > 19.195 fg; in this subgroup, to further differentiate control and anaplastic astrocytomas, *MMP9* < 0.775 fg clustered all control instances ($P = 1.000$).

Nomogram analysis, performed within the same data set and reported in Figure 5 confirmed that *PTEN* and *MMP9* expression analysis might be particularly helpful in the identification of anaplastic astrocytoma specimens having a 95% of probability ($P_{(\text{grade III})} = .95$) to correctly classify these samples, in correspondence of *MMP9*-normalized expression value of 19.195 fg, independently of *PTEN* expression level. Nomograms analysis with control and glioblastoma as target diagnostic classes showed less statistical significant probabilities ($P_{(\text{control})} = .60$ and $P_{(\text{grade IV})} = .55$).

To further elucidated if *PTEN* and *MMP9* expression had an expression trend that reflected the malignant grade of the specimens (i.e., normal, anaplastic astrocytomas,

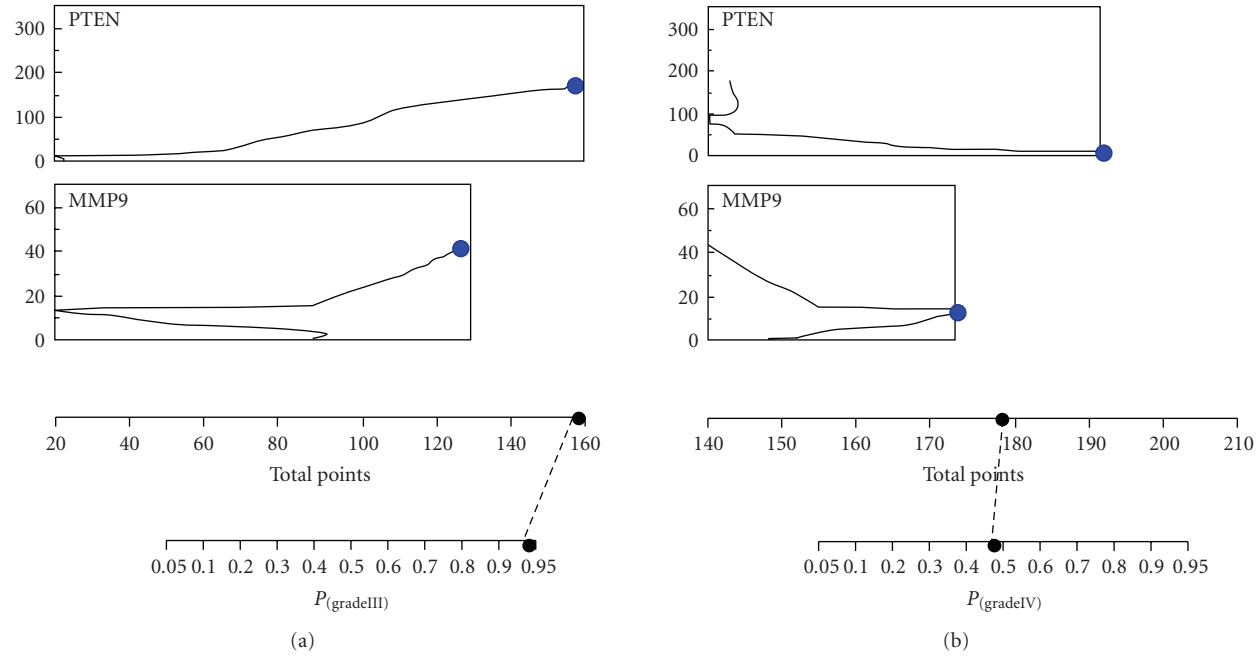

Figure 5: Nomogram analysis of *PTEN* and *MMP9* expression within the different WHO grades of malignancy (III, IV) of the astrocytomas specimens. Points and total points axes indicate the points attributed to each variable value and the sum of the points for each variable, respectively. *P* axes indicate the predicted probability that relates *PTEN* or *MMP9* quantitative expression to each WHO tumor malignancy grade.

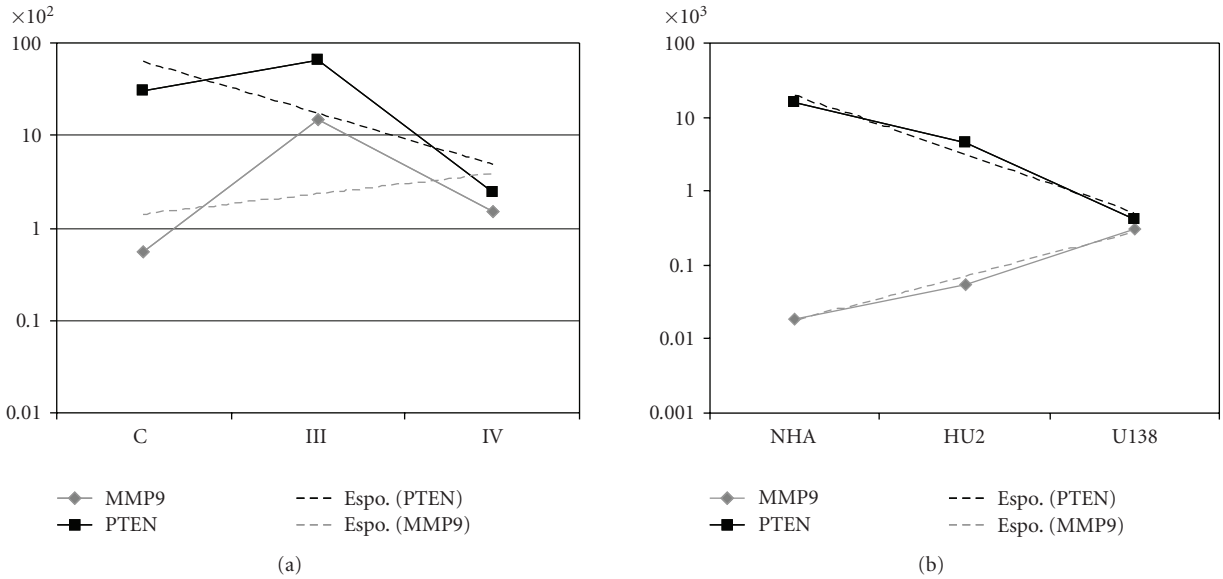

Figure 6: Statistical trends of *PTEN* (black dotted line) and *MMP9* (grey dotted line) expression in control (C), anaplastic astrocytomas (III) and glioblastoma multiforme (IV) specimens (Panel A), and in normal human astrocytes (NHA), glioma PRT-HU2 (HU2), and U138-MG (U138) cells (Panel B). Trends are calculated using average quantitative expression of *PTEN* and *MMP9*, and adopting exponential (Espo) models of prediction as follows: *PTEN* (C, III, IV average expression samples), $y = 2148e^{-1.29x}$; *MMP9* (C, III, IV), $y = 83716e^{0.50x}$; *PTEN* (NHA, HU2, U138), $y = 118596e^{-1.82x}$; *MMP9* (NHA, HU2, U138), $y = 42439e^{1.40x}$.

and glioblastoma multiforme), a statistical trend analysis was performed (Figure 6); the analysis reported in Panel A showed that *PTEN* and *MMP9* differences in their normalized expression clearly decreased following the malignant glioma grading, with the lowest values corresponding to glioblastoma multiforme specimens; similarly, the trend analysis, reported in Figure 6 Panel B, highlighted that, within the investigated cell lines, normal human astrocytes exhibited the largest differences in *PTEN* and *MMP9* expression levels, while, on the contrary, U138-MG cells,

isolated from a glioblastoma multiforme patient, showed nearly coincident *PTEN* and *MMP9* expression values; the glioblastoma derived PRT-HU2 cell line showed values of *PTEN* and *MMP9* expression trends, intermediate between NHA and U138-MG.

4. Discussion

The new challenge in cancer biology is to move from one purely morphological classification of cancer to one that is based on the integration of histological and molecular criteria [15]. Among several cancer specific investigated genes, the epidermal growth factor receptor (*EGFR*) plays a pivotal pathological role through the activation of downstream intracellular signalling pathways that can directly modulate cell proliferation, metastasis, and angiogenesis [8]. Glial tumors, in particular, due to processes of gene-amplification or mutation, showed altered *EGFR*-related functional pathways [3]. Within this context, in order to find clinically relevant correlations between gene expression and tumor malignant progression, a cohort of glioma specimens was analyzed for the expression of several genes, that is, *ADAM-17*, *PTEN*, *MMP9*, *EGFR*, and *HB-EGF*, indirectly involved in the *EGFR*-dependent signaling pathway, In fact, the concurrent measurement of the transcript levels of the different genes could potentially represent a useful tool to identify a dysregulation of receptor activation or of downstream signaling pathways or might also suggest functional links between these genes in pathological conditions [16].

Comparing a cohort of glioblastoma specimens and controls, only two genes, *ADAM-17* and *PTEN*, had expression levels that significantly changed between the two WHO classes; on the contrary, considering the expression of each transcript separately, we did not elucidate any association between clinical status and *EGFR*, *HB-EGF*, and *MMP9* expression profiles. In particular, the wide range of variation for the *EGFR* gene, found in glioblastoma specimens, was in partial agreement with previous studies carried out in glial tumor samples [8]. In general, nearly 50% of glioblastoma multiforme cases express amplified *EGFR*, and about 40% of them also express the constitutively activated mutated EGFRvIII isoform [11]. Since the primers we used in our experiments did not discriminate between *EGFR* and *EGFRvIII*, it is very likely that the *EGFR* mRNA levels found in our samples reflected the combined contribution of both the transcripts.

Since chemotherapic treatments enhance the EGFR-mediated proliferative responses via an increased *HB-EGF* expression and shedding [17], previous studies have suggested a prominent role for *HB-EGF* in tumorigenic processes. In fact, in glioma cell lines, the inducible expression of *EGFRvIII* can enhance *HB-EGF* expression and can activate *EGFR*-dependent pathways via a positive feedback autocrine loop [18]. The only previous published study, based on a semiquantitative assessment by Northern blot analysis, found an increased expression of *HB-EGF* in glioblastoma compared to control samples [9]. On the opposite, our data seemed to suggest that *HB-EGF* is not upregulated in glioblastoma; however, our results agreed with microarray gene expression profiles studies that showed no significant differences in *HB-EGF* expression between glioblastoma and control samples [19].

Recent mounting evidence showed that the expression of *MMP9* might play a critical role in brain neoplastic tissue invasion, metastasis, and angiogenesis [12]. Even if not completely statistically supported, our findings were in good agreement with a previous work showing an upregulation of *MMP9* mRNA levels in glioblastoma compared to controls and suggesting a close relationship between *MMP9* expression and tumor malignant progression [12].

Although *ADAM17* expression has been reported in normal human brain tissue and in cell lines [5], its expression at mRNA level has been poorly investigated in brain tumors. Functional studies in U373-MG glioma cells have demonstrated that cannabinoids induced cell proliferation through a two-step mechanism involving *ADAM17*-mediated shedding of *proHB-EGF* and subsequent *EGFR* stimulation [5]. Our finding that *ADAM17* mRNA levels in glioblastoma are statistically lower compared to controls is in contrast with a previous work that reported an increased expression of *ADAM17* in glioblastoma specimens [20]. This might reflect differences in tumor sampling or a consequence of glioblastoma multiforme cellular and molecular heterogeneity.

Our finding showing that glioblastoma expressed statistically significant lower *PTEN* mRNA levels compared to control samples confirmed previous reports [21], showing that *PTEN* expression variations were detectable only in a low fraction of anaplastic astrocytoma and were almost absent in low-grade brain tumors and controls. Taken together, these observations strengthen the hypothesis that an impairment of *PTEN* expression, together with a consequent aberrant activity of the PI3K-dependent pathway, might represent a typical hallmark of glioblastoma multiforme. A functional confirmation of this hypothesis was that, in a mouse astrocytoma model with genetic inactivation of the *Nf1* and *p53* tumor suppressor genes, the loss of *PTEN* heterozygosity and the Akt activation contributed to the brain tumor malignant progression [6].

Differently from the above mentioned investigated genes, the analysis of *PTEN* and *MMP9* expression, using a combination of unsupervised and supervised algorithms, provided interesting results: firstly, as reported in the dendrogram analysis, the expression profiling derived novel subsets of astrocytomas. This hierarchically clustering analysis clarified that tumor classification based even on a quantization of two genes could generate a patient stratification, clinically relevant and more informative than a single conventional histological classification. The *PTEN* and *MMP9* expression-generated subgroups produced also a different distribution of the patients according to their age: in particular subgroup IV-a, differently from IV-b, was enriched in age-class III patients (i.e., >61 years); this result might suggest that in glioblastoma multiforme tumor specimens *PTEN* and *MMP9* expression levels might be partly related with the elderly of the patients. On the contrary, in anaplastic astrocytoma and in control patients no association between age-related classes and *PTEN*/*MMP9* expression levels was evidenced. Furthermore, the originated dendrogram does

not reflect a classification of samples according to their anatomical tumor localization. However, in the light of the development of new pharmacological treatments, the identification of patient subsets with specific molecular signatures within tumor malignancy grades is becoming more and more relevant [22]. A finer analysis of *PTEN* and *MMP9* expression was also employed to derive a parsimonious classification tree of the investigated samples into their tumor malignancy grades. Specific *PTEN* and *MMP9* expression values significantly addressed the specimens into a specific diagnostic class, that is, glioblastoma or anaplastic astrocytomas. However, the significance and the sensitivity of this classification might be further refined with the increasing of specimens and through the identification of novel tumor-diagnostic markers. Basing on the average expression of *PTEN* and *MMP9*, the observed statistical trends clearly differentiate the control, anaplastic astrocytomas, and glioblastoma multiforme diagnostic classes; a similar expression trend for *PTEN* and *MMP9* genes was documented comparing normal versus astrocytic tumor cell lines. These results, in particular, reinforced the concept that anaplastic astrocytomas were intermediate-grade tumors, showing detectable mitotic activity, absent in low-grade astrocytomas, but not necrosis and prominent vascular proliferation, characteristic of glioblastoma multiforme [23, 24].

An additional interesting finding emerging from our study was the significant negative correlation between *PTEN* and *MMP9* mRNA expression in glioblastoma multiforme. Notably, not only was this negative correlation absent in anaplastic astrocytoma samples, but it was reversed in control samples. It was evident that differences in *PTEN* gene expression mainly account for these correlations because its levels in glioblastoma were significant higher compared to anaplastic astrocytoma samples, whilst no statistical difference was found for *MMP9* mRNA levels. The positive correlation between *PTEN* and *MMP9* in controls is derived essentially from an overexpression of *PTEN* rather than a low expression of *MMP9* compared to glioblastoma. The functional significance of these correlations is currently unknown, and future functional studies aimed at elucidating possible interplays of these genes in glioblastoma are clearly warranted. The negative correlation in glioblastoma between *MMP9* and *PTEN* could imply a functional interplays between these two genes, as already documented. It has been reported that *PTEN* modulates the expression and secretion of MMP2 and MMP9, thereby modifying tumor cell invasiveness [9, 25]. Notably, recent reports have clearly demonstrated that, in glioblastoma, *PTEN* may regulate migration via a PI3K-independent pathway [26]. In this model, the lack or functional loss of *PTEN* not only potentiates the migration induced by EGFR- and beta-integrin-dependent pathways but also enhances cell migration via a still largely unclear mechanism. On this regard, a recent report suggested that integrins could be a converging point in the mechanism supporting tumor invasion and migration of cancer cells with *PTEN* loss and *MMP9* overexpression.

The intrinsic genetic heterogeneity and redundant overlapping aberrant signalling transduction pathways underlie the failure of monotherapies in glioblastoma [8]. Therefore a sensitive and reliable method to measure gene expression, such as Real-time PCR, may greatly ameliorate diagnostic tools and eventually address the pharmacological approach using multitarget kinase inhibitors or combination of therapies based on multiple single-targeted receptor or intracellular kinase inhibitors. Some researchers have proposed that the combination of *PTEN* loss and *EGFR* hyperfunctionality could be predictive of the ineffectiveness of therapies with *EGFR* inhibitors [4] because these two pathways might synergize to enhance glioblastoma malignancy. This hypothesis has been elegantly supported by the recent observation that the pharmacological inhibition of PI3K-alpha and mTOR augments the antiproliferative activity of the EGFR inhibitor erlotinib in glioblastoma cell lines [7]. The inverse correlation between *PTEN* and *MMP9* expression reported here raised the issue whether the concomitant hyperactivation of the PI3K-alpha and MMP9-dependent pathways might be instrumental in devising or refining combined pharmacological therapies in glioblastoma. The modest efficacy of mTOR inhibitors alone in clinical trials was greatly enhanced when these compounds were administered in combination with the EGFR inhibitor Gefitinib [27]. Although monotherapy regimens with MMPs inhibitors in clinical trials have been quite disappointing, the relevance of MMPs as valid target has been reevaluated by the recent finding that the combined use of MMPs, COX2, and EGFR inhibitors reduced human breast cancer tumor growth [11]. We therefore speculate that the pivotal role of MMPs in glioma invasion and angiogenesis deserves future in vitro and in vivo experiments using MMP inhibitors in combination with PI3K inhibitors alone or with these latter compounds plus EGFR inhibitors.

The analyses of gene expression at transcriptional level in biopsy tissue samples are instrumental in delineating abnormal gene expression signature of brain tumors, but it should be mentioned that these studies suffer some pitfalls and limitations: in particular, the use of supervised approaches, based on the assumption that the grouping (i.e., the histological tumor diagnoses) is correct, may not be a valid assumption for all the clinical cases examined; additionally, the intrinsic heterogeneity of glioblastoma, together with the presence of nontumor cells in the samples, probably accounts for the variability found in transcripts levels and may represent a critical factor and a limitation in the interpretation of our results. From a technical point of view, a main difference of our contribution, compared to other reports, deals with the criteria adopted to express transcript levels in the investigated specimens. The majority of clinical gene expression profile studies performed by Real-time PCR normalized data using an internal housekeeping gene as a reference, but great caution in choosing this normalization method is necessary especially when analyzing tumor biopsy samples [28]. The tumorigenic process itself, via genomic mutations or amplifications, could induce modifications of housekeeping genes levels [29], and hence the choice of unreliable housekeeping genes may lead to interpretation errors and bias in experimental results [30]. Our attempts to use *GAPDH, ACTB*, and *HPRT* as reference genes were unsuccessful due to the great variations among

all the samples (data not shown); therefore, we decided to express gene expression as absolute amount of femtograms (fg) of transcripts, normalized to the total amount of RNA employed, through accurate quantification using the combination of spectrofotometric and fluorimetric approaches.

In conclusion, the combined analysis of the transcripts of *PTEN* and *MMP9* genes in biopsy specimens could represent a reliable diagnostic and prognostic marker of human glial tumor. Further epidemiological and functional in vitro studies are required to establish the reliability of *PTEN* and *MMP9* genes as possible valid molecular targets in the pharmacological strategies aimed at controlling human glioma malignant progression.

Acknowledgments

This study was supported by grants from the Italian MIUR, "Progetti di Ricerca di Rilevante Interesse Nazionale (2005)." A. A. is granted by Fondo Sociale Europeo (F.S.E.). The authors are particularly grateful to Dr. Eugenio Benericetti (Azienda Ospedaliera di Parma, Italy) for providing WHO graded glioma specimens. Orange Software is released under General Programming License (GPL). The authors are therefore particularly grateful to Orange Program's authors, Demsar J, Zupan B, Leban G: (2004) Orange: From Experimental Machine Learning to Interactive Data Mining, White Paper (http://www.ailab.si/orange/), Faculty of Computer and Information Science, University of Ljubljana (Slovenia).

References

[1] D. N. Louis, "Molecular pathology of malignant gliomas," *Annual Review of Pathology*, vol. 1, pp. 97–117, 2006.

[2] H. Ohgaki and P. Kleihues, "Genetic pathways to primary and secondary glioblastoma," *American Journal of Pathology*, vol. 170, no. 5, pp. 1445–1453, 2007.

[3] S. Higashiyama and D. Nanba, "ADAM-mediated ectodomain shedding of HB-EGF in receptor cross-talk," *Biochimica et Biophysica Acta*, vol. 1751, no. 1, pp. 110–117, 2005.

[4] S. Miyamoto, H. Yagi, F. Yotsumoto, T. Kawarabayashi, and E. Mekada, "Heparin-binding epidermal growth factor-like growth factor as a novel targeting molecule for cancer therapy," *Cancer Science*, vol. 97, no. 5, pp. 341–347, 2006.

[5] S. Hart, O. M. Fischer, and A. Ullrich, "Cannabinoids induce cancer cell proliferation via tumor necrosis factor α-converting enzyme (TACE/ADAM17)-mediated transactivation of the epidermal growth factor receptor," *Cancer Research*, vol. 64, no. 6, pp. 1943–1950, 2004.

[6] C.-H. Kwon, D. Zhao, J. Chen, et al., "Pten haploinsufficiency accelerates formation of high-grade astrocytomas," *Cancer Research*, vol. 68, no. 9, pp. 3286–3294, 2008.

[7] Q.-W. Fan, C. K. Cheng, T. P. Nicolaides, et al., "A dual phosphoinositide-3-kinase α/mTOR inhibitor cooperates with blockade of epidermal growth factor receptor in PTEN-mutant glioma," *Cancer Research*, vol. 67, no. 17, pp. 7960–7965, 2007.

[8] J. B. Johnston, S. Navaratnam, M. W. Pitz, et al., "Targeting the EGFR pathway for cancer therapy," *Current Medicinal Chemistry*, vol. 13, no. 29, pp. 3483–3492, 2006.

[9] M.-S. Kim, M.-J. Park, E.-J. Moon, S.-J. Kim, C.-H. Lee, and H. Yoo, "Hyaluronic acid induces osteopontin via the phosphatidylinositol 3-kinase/Akt pathway to enhance the motility of human glioma cells," *Cancer Research*, vol. 65, no. 3, pp. 686–691, 2005.

[10] T. Hastie, R. Tibshirani, D. Botstein, and P. Brown, "Supervised harvesting of expression trees," *Genome Biology*, vol. 2, no. 1, article research0003.1-0003.12, 2001.

[11] I. K. Mellinghoff, M. Y. Wang, I. Vivanco, et al., "Molecular determinants of the response of glioblastomas to EGFR kinase inhibitors," *The New England Journal of Medicine*, vol. 353, no. 19, pp. 2012–2024, 2005.

[12] K. Komatsu, Y. Nakanishi, N. Nemoto, T. Hori, T. Sawada, and M. Kobayashi, "Expression and quantitative analysis of matrix metalloproteinase-2 and -9 in human gliomas," *Brain Tumor Pathology*, vol. 21, no. 3, pp. 105–112, 2004.

[13] P. Kleihues and W. K. Cavenee, *World Health Organization Classification of Tumors of the Nervous System*, Lyon, France, 2000.

[14] M. Paolillo, A. Barbieri, P. Zanassi, and S. Schinelli, "Expression of endothelins and their receptors in glioblastoma cell lines," *Journal of Neuro-Oncology*, vol. 79, no. 1, pp. 1–7, 2006.

[15] D. N. Louis, E. C. Holland, and J. G. Cairncross, "Glioma classification: a molecular reappraisal," *American Journal of Pathology*, vol. 159, no. 3, pp. 779–786, 2001.

[16] Y. Liang, M. Diehn, N. Watson, et al., "Gene expression profiling reveals molecularly and clinically distinct subtypes of glioblastoma multiforme," *Proceedings of the National Academy of Sciences of the United States of America*, vol. 102, no. 16, pp. 5814–5819, 2005.

[17] F. Wang, R. Liu, S. W. Lee, C. M. Sloss, J. Couget, and J. C. Cusack, "Heparin-binding EGF-like growth factor is an early response gene to chemotherapy and contributes to chemotherapy resistance," *Oncogene*, vol. 26, no. 14, pp. 2006–2016, 2007.

[18] D. B. Ramnarain, S. Park, D. Y. Lee, et al., "Differential gene expression analysis reveals generation of an autocrine loop by a mutant epidermal growth factor receptor in glioma cells," *Cancer Research*, vol. 66, no. 2, pp. 867–874, 2006.

[19] D. S. Rickman, M. P. Bobek, D. E. Misek, et al., "Distinctive molecular profiles of high-grade and low-grade gliomas based on oligonucleotide microarray analysis," *Cancer Research*, vol. 61, no. 18, pp. 6885–6891, 2001.

[20] D. Wildeboer, S. Naus, Q.-X. A. Sang, J. W. Bartsch, and A. Pagenstecher, "Metalloproteinase disintegrins ADAM8 and ADAM19 are highly regulated in human primary brain tumors and their expression levels and activities are associated with invasiveness," *Journal of Neuropathology and Experimental Neurology*, vol. 65, no. 5, pp. 516–527, 2006.

[21] C. B. Knobbe, A. Merlo, and G. Reifenberger, "Pten signalling in gliomas," *Neuro-Oncology*, vol. 4, no. 3, pp. 196–211, 2002.

[22] G. N. Fuller, K. R. Hess, C. H. Rhee, et al., "Molecular classification of human diffuse gliomas by multidimensional scaling analysis of gene expression profiles parallels morphology-based classification, correlates with survival, and reveals clinically-relevant novel glioma subsets," *Brain Pathology*, vol. 12, no. 1, pp. 108–116, 2002.

[23] K. Ichimura, H. Ohgaki, P. Kleihues, and V. P. Collins, "Molecular pathogenesis of astrocytic tumours," *Journal of Neuro-Oncology*, vol. 70, no. 2, pp. 137–160, 2004.

[24] B. K. Ahmed Rasheed, R. N. Wiltshire, S. H. Bigner, and D. D. Bigner, "Molecular pathogenesis of malignant gliomas," *Current Opinion in Oncology*, vol. 11, no. 3, pp. 162–167, 1999.

[25] K. Furukawa, Y. Kumon, H. Harada, et al., "PTEN gene transfer suppresses the invasive potential of human malignant

gliomas by regulating cell invasion-related molecules," *International Journal of Oncology*, vol. 29, no. 1, pp. 73–81, 2006.

[26] M. Raftopoulou, S. Etienne-Manneville, A. Self, S. Nicholls, and A. Hall, "Regulation of cell migration by the C2 domain of the tumor suppressor PTEN," *Science*, vol. 303, no. 5661, pp. 1179–1181, 2004.

[27] S. Sathornsumetee, D. A. Reardon, A. Desjardins, J. A. Quinn, J. J. Vredenburgh, and J. N. Rich, "Molecularly targeted therapy for malignant glioma," *Cancer*, vol. 110, no. 1, pp. 12–24, 2007.

[28] C. Tricarico, P. Pinzani, S. Bianchi, et al., "Quantitative real-time reverse transcription polymerase chain reaction: normalization to rRNA or single housekeeping genes is inappropriate for human tissue biopsies," *Analytical Biochemistry*, vol. 309, no. 2, pp. 293–300, 2002.

[29] S. Waxman and E. Wurmbach, "De-regulation of common housekeeping genes in hepatocellular carcinoma," *BMC Genomics*, vol. 8, pp. 243–250, 2007.

[30] J. L. Aerts, M. I. Gonzales, and S. L. Topalian, "Selection of appropriate control genes to assess expression of tumor antigens using real-time RT-PCR," *BioTechniques*, vol. 36, no. 1, pp. 84–91, 2004.